Environ. Sci. Technol. **2007**, *41,* 1934−1941

Sorption and Inhibited Dehydrohalogenation of 2,2-Dichloropropane in Micropores of Dealuminated Y Zeolites†

HEFA CHENG AND MARTIN REINHARD*

Department of Civil and Environmental Engineering, Stanford University, Stanford, California 94305-4020

Contaminant transformation rates in the subsurface can be slowed by sorption onto geosorbents. We evaluated the effect of micropore sorption on contaminant transformation in a model system consisting of dealuminated Y zeolites and 2,2-dichloropropane (2,2-DCP). 2,2-DCP dehydrochlorinates in water to 2-chloropropene (2-CP) at a rate of 2.93 $\times$ 10^{-4} min^{-1} at 24 °C. The Y zeolites used range from hydrophilic (CBV-300) to hydrophobic (CBV-720 and CBV-780). Wet zeolite samples were loaded with 2,2-DCP at 24 °C and reacted at 50 °C for 10 h. Results show that the hydrophobic zeolites (CBV-720 and CBV-780) sorbed nearly 900 times more 2,2-DCP than the hydrophilic CBV-300 under wet conditions. 2,2-DCP transformed less when sorbed in micropores of CBV-720 (6.3%) and CBV-780 (5.0%) than in micropores of CBV-300 (81.5%), and significantly less than in water (>99.85%). Inhibition in hydrophobic micropores is interpreted as lack of water solvating the transition state of 2,2-DCP dehydrohalogenation and the H^+ and Cl^- formed. Near the micropore openings, the transformation was relatively fast, consistent with greater abundance of water associated with the hydrophilic edge sites. These results indicate that in the subsurface the half-lives of reactive organic contaminants may be longer than predicted from bulk water data.

Introduction

Field and laboratory data indicate that sorption can inhibit transformation of reactive organic contaminants (*1*−*4*). In an exploratory study, we have postulated that inhibition may be caused by sorption in hydrophobic micropores (≤2 nm) of geosorbents (soils, sediments, and aquifer materials) (*3*). In geosorbents with low organic carbon contents (<0.1%), micropores can serve as a sink for small but significant amounts of volatile organic compounds (VOCs), such as trichloroethylene (TCE) and ethylene dibromide (EDB) (*3*−*8*). Sorption and desorption characteristics of VOCs in micropores of geosorbents and synthetic minerals (e.g., silica gels and zeolites) were previously studied (*3*, *5*−*9*).

To predict the fate of reactive organic contaminants sorbed on geosorbents, it is necessary to understand the reactivity in each compartment. Sorption on geosorbents can occur by (i) partitioning into entrapped nonaqueous-phase liquids (NAPLs; e.g., solvents, oils, and tars) or amorphous soil organic matter (SOM), (ii) adsorption on surfaces of minerals, condensed SOM, or carbonaceous combustion residues (e.g., chars, soot, and ashes), or (iii) adsorption in micropores of minerals or dense SOM (*10*). The availability of water can affect contaminant transformation reaction, as illustrated in Figure 1 with 2,2-dichloropropane (2,2-DCP). Organic compounds partitioned in amorphous SOM are excluded from water (and hydroxide ions), and therefore they hydrolyze more slowly when sorbed than in bulk water. This was shown for hydrolysis of 2,4-dichlorophenoxyacetic acid octyl ester (*1*) and chlorpyrifos (*2*) sorbed in humic substances. By contrast, the hydrolysis rates of organophosphorothiate esters, haloalkanes, and several halogenated pesticides, which were sorbed on the external surfaces of low-carbon sediments, were not significantly affected (*11*, *12*). Although micropores are known sinks for organic contaminants in geosorbents, the effect of micropore sorption on contaminant transformation is largely unknown.

In a recent study, we observed that sorption in micropores of an aquifer sediment slows the dehydrohalogenation of 2,2-DCP (*3*). In this study, we demonstrate sorption in hydrophobic micropores can inhibit hydrolytic transformation (or transformations requiring water in general) using hydrophilic (CBV-300) and hydrophobic (CBV-720 and CBV-780) dealuminated Y zeolites as model sorbents. The dealuminated Y zeolites have identical micropore structures and volumes, and they have defined surface properties (*13*). The Si/Al ratios of CBV-300, CBV-720, and CBV-780 are 2.6, 15, 40, whereas their monovalent surface cation densities are 2.07, 0.42, 0.16 sites/nm^2, respectively (*14*). Micropores in CBV-300 are categorized as hydrophilic; those in CBV-720 and CBV-780 are characterized as hydrophobic (*14*, *15*).

2,2-DCP was chosen as the model reactant because it dehydrochlorinates in water relatively quickly to 2-chloropropene (2-CP) at room temperature, and its reaction rate is known and pH-independent (*16*, *17*). Dehydrohalogenation of 2,2-DCP follows the E_1 mechanism (*17*) in a two-step process with elimination ionization (rate-determining step) followed by deprotonation (Figure 1a). Reactions that involve the formation of charged species are typically extremely endothermic in the gas phase, but they may become spontaneous in water because solvation facilitates charge separation by stabilizing the transition state (*18*). In the absence of solvation, reactions involving a charge separation step tend to proceed slower and sometimes follow different reaction mechanisms than in solution (*19*, *20*). Lack of water and steric hindrance in the confinement of micropores are hypothesized to limit solvation of the transition state and the ionic species, thereby inhibiting contaminant transformation.

Figure 2 schematically illustrates the hypothesized effect of micropore sorption on hydrolytic transformation of 2,2-DCP. Several studies have established that sorption of VOCs in hydrophobic micropores of silica gels (*21*), dealuminated Y zeolites (*14*), and graphite (*22*, *23*) involves displacement of loosely bound water. The process is driven primarily by the negative enthalpy of transferring loosely bound water to the bulk phase (*14*, *21*). 2,2-DCP molecules sorbed in micropores form micro-clusters of neat organic liquid (*24*, *25*) that contact only nonpolar siloxane walls or tightly bound water. Under these conditions, transformations that require the solvation of a charged transition state and ionic products, such as dehydrodehalogenation and hydrolysis reactions, will be inhibited. The inhibiting effect is expected to be diminished near the pore openings by the relatively abundant water sorbed at polar edge sites. Polar surface sites exist even

† Abstract published in Extended Abstracts of the 231st National Meeting of the American Chemical Society.

* Corresponding author phone: (+1) 650 723-0308; fax: (+1) 650 723-7058; e-mail: reinhard@stanford.edu.

10.1021/es062332v CCC: $37.00
Published on Web 02/15/2007

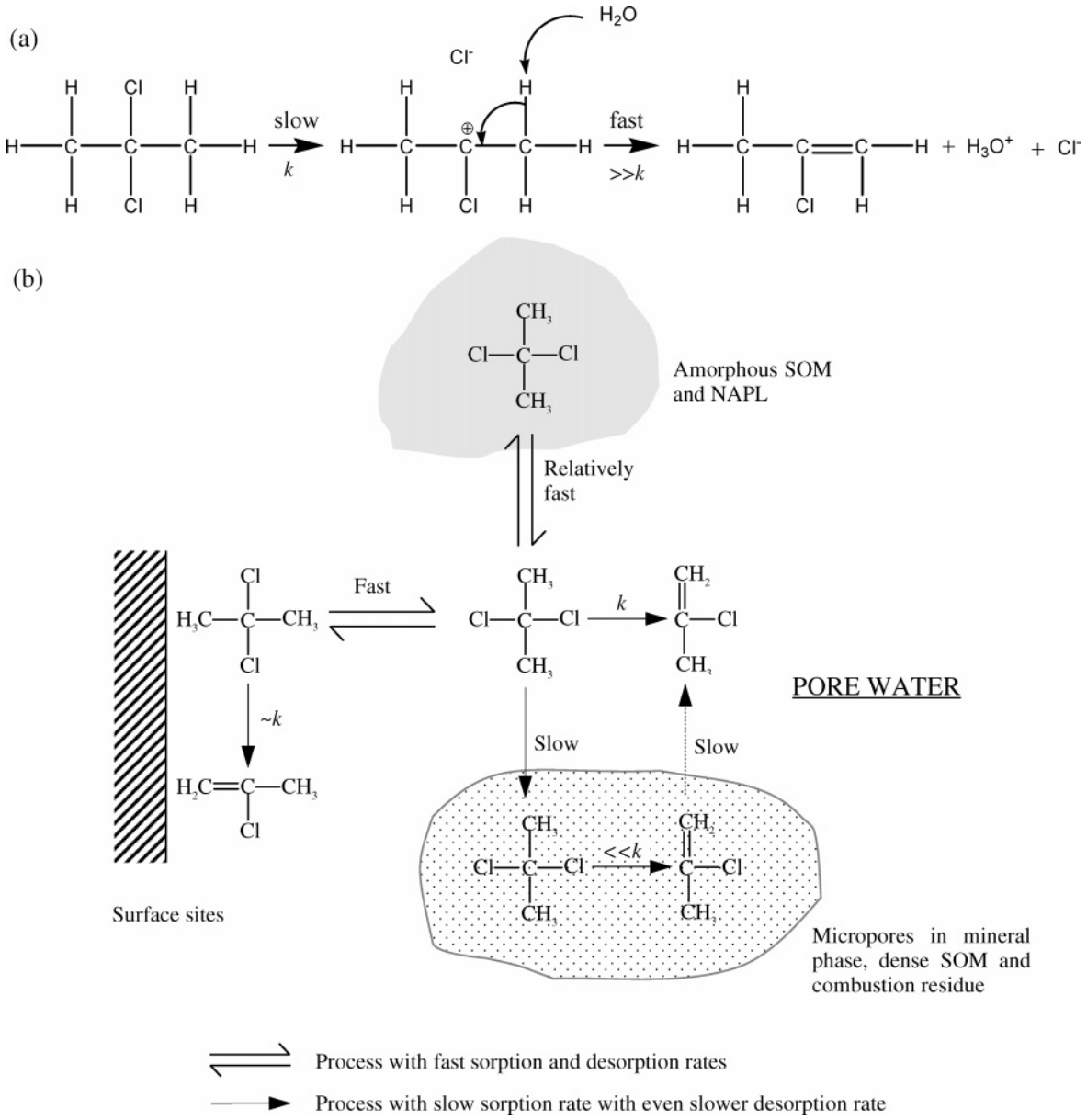

FIGURE 1. Schematic illustration of the transformation of a reactive organic compound, 2,2-DCP. (a) Reaction mechanism in bulk water. (b) Transformation in a typical soil environment: surface adsorption and partitioning into exposed amorphous SOM (and NAPL) and the corresponding desorption processes typically occur in seconds to minutes (depending on the sizes of the SOM particles or the NAPL) (*10, 33*), while adsorption in and desorption from micropores of minerals, condensed SOM, and combustion residue occur on the time scale of hours to months (*5, 8, 9, 10*). 2,2-DCP sorbed on external surfaces or partitioned in amorphous SOM exchanges relatively rapidly with the aqueous phase, and the transformation is not significantly impacted. In contrast, the slow-releasing micropore-sorbed fraction is not readily available for chemical reactions occurring in the aqueous phase.

in hydrophobic minerals such as talc, because of surface defects and broken bonds, particularly at the edge surfaces (*26*, *27*).

Materials and Methods

Materials. Samples of binder-free dealuminated Y zeolites (CBV-300, CBV-720, and CBV-780) were obtained in powder form (1−2 μm diameter crystals) from Zeolyst (Valley Forge, PA) and were used as received. The crystallinity and structure of the dealuminated Y zeolites are close to that of the non-dealuminated parent zeolites (*13*, *14*). Y zeolites have the FAU structure with pores running mutually perpendicular in the *x*, *y*, and *z* planes. The pore diameter is large at 7.4 Å with 12 Å cavities. Properties of the zeolites used were summarized previously (*14*). After being hydrated for at least 3 months at 100% RH and room temperature (24 ± 1 °C), the water contents of all three zeolites were 0.45 g/g (*14*), only slightly lower than the theoretical void volume of 0.48 mL/g. Besides 2,2-DCP, TCE was used as a nonreactive reference sorbate to study desorption behavior from CBV-300. 2,2-DCP with a purity of 99.3% (Lot 11231TA), 2-CP with a purity of 97.4% (Lot 52900/1), and TCE (99.5+% purity, ACS reagent-grade) were obtained from Sigma-Aldrich (Milwaukee, WI), and all chemicals were used as received. Selected physico-chemical properties of TCE, 2,2-DCP, and 2-CP and their diffusivities in air and bulk water are summarized in Table 1.

Transformation Experiments. Sorption and desorption experiments with TCE and 2,2-DCP were conducted using the experimental apparatus and procedures previously described (*3*, *14*). In brief, wet zeolite was first packed into a preweighted column with the zeolite mass determined by

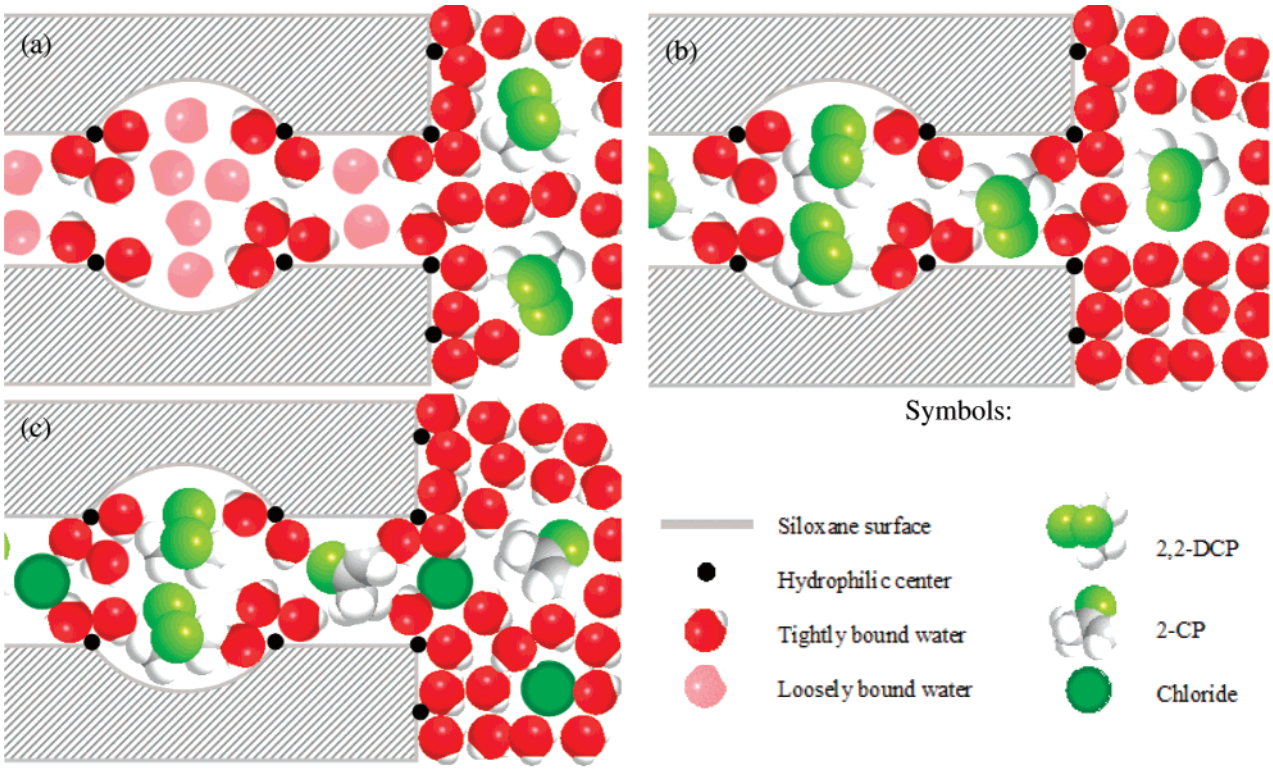

FIGURE 2. Schematic illustration of sorption and dehydrohalogenation of 2,2-DCP molecules in a water-filled hydrophobic micropore with a moderate density of hydrophilic centers. (a) Water molecules are tightly bound to the hydrophilic centers through both coordination to surface cations and hydrogen bonding to surface hydroxyl groups in the hydrophilic pore spaces (*34*), while they form disordered clusters with limited intermolecular hydrogen bonding and weak hydrogen bonds with the siloxane surface in the hydrophobic pore spaces (*35*), which are known as "loosely bound" water. (b) 2,2-DCP adsorbs in the hydrophobic pore spaces through displacing the loosely bound water (*14*). (c) After a long reaction time, 2,2-DCP molecules residing near the pore openings and the hydrophilic micropore spaces undergo hydrolytic transformation to a greater extent compared to those deeper in the hydrophobic micropore spaces, which are mostly surrounded by other 2,2-DCP molecules, tightly bound water, and the hydrophobic siloxane surface.

TABLE 1. Physicochemical Properties of TCE, 2,2-DCP, and 2-CP, and Their Diffusivities in Air and Bulk Water at 24 °C

compound	TCE	2,2-DCP	2-CP
molecular structure	$CHCl{=}CCl_2$	$CH_3CCl_2CH_3$	$CH_2{=}CClCH_3$
molecular weight	131.4	113.0	76.5
density,[a] g/cm^3	1.46	1.11	0.91
molar volume,[b] cm^3/mol	89.9	101.6	84.1
dipole moment,[c] D	0.77	2.62	1.65
log K_{ow}[a]	2.42	2.92	2.00
solubility in water at 25 ˚C,[a] mg/L	1280	391	2600
major hydrolysis product	N/A[d]	2-CP	N/A
hydrolysis rate at pH 7 and 24 °C,[e] 1/min	1.07×10^{-12}	3.18×10^{-4}	N/A
molecular diffusivity in air at 24 °C,[f] cm^2/s	1.48×10^{-2}	1.40×10^{-2}	1.49×10^{-2}
molecular diffusivity in bulk water at 24 °C,[g] cm^2/s	9.40×10^{-6}	8.64×10^{-6}	9.79×10^{-6}

[a] From ref *30*. [b] Calculated from molecular weight and density at standard conditions. [c] From ref *31*. [d] N/A: not available. [e] From ref *16*. [f] Estimated from Brokaw equation (*32*). [g] Estimated from Wilke–Chang equation (*32*).

weight difference. The column was then equilibrated with water vapor by passing a humidified (100% RH) helium stream through the column for at least 2 h. To load 2,2-DCP onto the sorbent, a humidified (100%) helium stream laden with 2,2-DCP vapor ($P/P_0 = 0.147$) at 24 °C was passed through the column at 1.00 mL/min (~1.4 pore volume/min) until breakthrough. The column was then sealed off and heated at 50 °C for 10 h. After heat treatment the column was cooled to room temperature, re-connected, and purged with a humidified (100% RH) helium stream at 1.00 mL/min. During desorption, 2,2-DCP and 2-CP in the column effluent were analyzed using an on-line gas chromatograph equipped with a flame ionization detector and an electron capture detector. Once the VOC concentrations decreased to relatively low levels, the column temperature was increased stepwise to accelerate desorption, as reported elsewhere (*3*, *5*). TCE sorption and desorption were conducted similarly with wet CBV-300 except that P/P_0 was 0.136. At 100% RH conditions in micropores are the same as if the microporous solids are immersed in water; findings therefore should also apply to both groundwater aquifers and the unsaturated zone with gas-phase RH close to 100%.

Data Evaluation. The mass of 2,2-DCP retained in the column was calculated from the difference between the areas above the breakthrough curves with and without the column (*14*). Desorption profiles were evaluated using a radial diffusion model (RDM), either alone or in conjunction with the advection–dispersion equation (ADE), following previously reported procedures (*3*, *7*). On wet CBV-720 and CBV-780, the mass of 2,2-DCP external to micropores (i.e., in

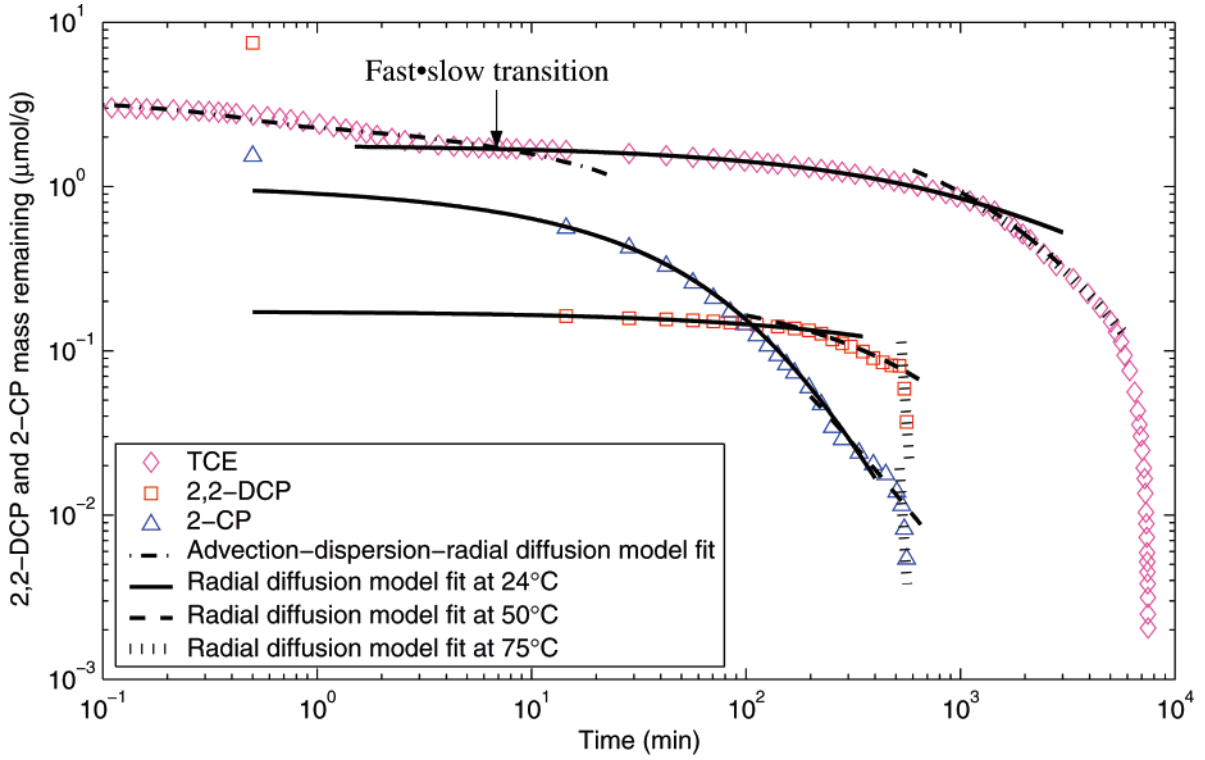

FIGURE 3. Mass remaining profiles of TCE, 2,2-DCP, and 2-CP (formed from sorbed 2,2-DCP) on wet CBV-300 after 10 h reaction at 50 °C; lines represent model fits. Data were obtained from two separate column experiments (preloaded with vapor of TCE and 2,2-DCP, respectively). The exact transition from fast- to slow-desorption was not observed for 2,2-DCP and 2-CP because it was not possible to collect data between 0.5 and 14.5 min using the discrete sampling method (*3*).

interparticulate void space, adsorbed on external surface, and partitioned in adsorbed water film) was insignificant compared to that sorbed in the micropores. Therefore, 2,2-DCP masses in micropores of wet CBV-720 and CBV-780 were approximated as being equal to the total masses (Figure S1, Supporting Information). Wet CBV-300 retained too little VOCs for quantification by evaluating breakthrough curves. Therefore, the amounts of TCE and 2,2-DCP sorbed in the micropores were quantified by integrating the slow-desorbing flux over time (Figure 3) (*14*). Volumes of the micropores occupied by 2,2-DCP and water were calculated based on Gurvitsch's rule (*24*), as discussed previously (*3*, *14*).

The pseudo first-order dehydrohalogenation rate (at 24 °C) and the activation energy of 2,2-DCP have been determined in bulk water as 2.93×10^{-4} min^{-1} and 111.1 ± 2.0 kJ/mol, respectively (*16*). The respective half-lives of 2,2-DCP transformation in bulk water at 24 °C and 50 °C are 39.5 and 1.06 h, respectively. For 2,2-DCP dehydrohalogenation, treatment at 50 °C for 10 h corresponds to 9.4 half-lives in bulk water, or 99.8565% transformation (note: reference *3* erroneously specifies 99.9948%). In all cases, most of the 2,2-DCP and 2-CP masses (88.7−99.9%) were removed during the isothermal stage (at 24 °C, <0.85 half-life) of desorption. Therefore, 2,2-DCP transformation during the desorption process was deemed insignificant. The influence of micropore sorption on 2,2-DCP transformation was evaluated by comparing the percentage transformed in the sorbed state to the predicted transformation in bulk water.

Results and Discussion

1. 2,2-DCP Adsorption. Table 2 summarizes the quantities of water and 2,2-DCP sorbed in micropores of the wet zeolites at 100% RH and a 2,2-DCP relative pressure (P/P_0) of 0.147. Observations with 2,2-DCP parallel those of TCE studied earlier (*14*): the hydrophobic zeolites (CBV-720 and CBV-780) sorbed nearly 900 times more 2,2-DCP than the hydrophilic CBV-300, and uptake of 2,2-DCP in the water-filled micropores would require expulsion of an equal volume of loosely bound water for steric reasons. The volume of loosely bound water decreases with surface cation density, which explains the low 2,2-DCP uptake by CBV-300 (2.07 cationic sites/nm^2). The slightly higher uptake of 2,2-DCP by wet CBV-720 (0.42 cationic sites/nm^2) than by wet CBV-780 (0.16 cationic sites/nm^2) contradicts this trend, perhaps because 2,2-DCP, with its relatively high dipole moment (2.62 D vs 0.77 D of TCE), displaced water more effectively than TCE.

2. Transformation of 2,2-DCP in the Hydrophilic Zeolite CBV-300. Figure 3 shows the mass remaining profiles of two wet CBV-300 columns each loaded with TCE and 2,2-DCP, respectively. TCE desorption exhibited the two-stage behavior characteristic of microporous solids (*3*, *5*−*9*) with the transition from fast- to slow-desorbing fractions occurring at approximately 7 min (as indicated by the arrow in Figure 3). TCE removal in the first desorption stage was fitted to the ADE coupled with the RDM. Figure 3 reveals that only a fraction of the micropore-sorbed 2,2-DCP transformed to 2-CP; the transformation would have been complete in bulk water under identical conditions. The mass remaining of both compounds decreased rapidly (99% and 82% for 2,2-DCP and 2-CP, respectively) between 0.5 and 14.5 min but only slowly thereafter, indicating the transition from first to second stage (micropore-limited desorption) occurred within this time span. For the stage of micropore desorption, the mass remaining profiles of TCE, 2,2-DCP, and 2-CP fitted the RDM with a γ-distribution of diffusion rate constants. Stepwise temperature increases caused desorption fluxes to spike (Figure S2, Supporting Information), consistent with higher micropore diffusion rates at higher temperatures (*3*, *5*).

Table 3 summarizes the micropore diffusion rate constants (D/R^2) obtained by fitting the 24 °C and 50 °C desorption

TABLE 2. Summary of 2,2-DCP Sorbed in Micropores of Wet CBV-300, CBV-720, and CBV-780 at a Relative Pressure of 0.147, Water Remaining after 2,2-DCP Sorption, and 2-CP Formed after Reaction at 50 °C for 10 h

zeolite	CBV-300	CBV-720	CBV-780
mass of 2,2-DCP sorbed, μmol/g	N/A[a]	617	583
volume of 2,2-DCP sorbed,[b] μL/g	6.9×10^{-2} [c]	63	59
initial water volume,[d] μL/g	450	450	451
volume of water displaced,[e] μL/g	6.9×10^{-2}	63	59
volume of water remaining after 2,2-DCP sorption,[f] μL/g	450	387	392
mass of 2,2-DCP desorbed, μmol/g	0.13[g]	569[h]	553[h]
mass of 2-CP desorbed, μmol/g	0.55[g]	38[h]	29[h]
mass of 2,2-DCP + 2-CP desorbed, μmol/g	0.68	607	582
overall mass balance, %	–	98.4	99.8
2,2-DCP remaining, %	18.5	93.7	95.0
2,2-DCP transformed, %	81.5	6.3	5.0

[a] N/A: Value cannot be quantified from the 2,2-DCP breakthrough curve because the mass residing outside of micropores is significant relative to that sorbed in the micropores. [b] Calculated from micropore-sorbed 2,2-DCP by assuming the density is that of the bulk liquid. [c] Based on the masses of 2,2-DCP and 2-CP removed in the slow-desorbing fraction from wet zeolites CBV-300, which had been exposed to 2,2-DCP vapor. [d] Previously determined by dehydration (*14*). [e] Calculated as the volume of 2,2-DCP sorbed because 2,2-DCP is incompressible and the zeolite framework is not expansible under the experimental conditions. [f] Calculated as the differences between the initial water volumes and the volumes of water displaced. [g] Calculated from the masses of 2,2-DCP and 2-CP removed in the slow-desorbing fraction. [h] All 2,2-DCP and 2-CP masses were assumed to reside in the zeolite micropores.

TABLE 3. Best-Fit Micropore Diffusion Rate Constants (D/R^2) and Shape Factors (η) of TCE, 2,2-DCP, and 2-CP in Micropores of the Three Dealuminated Y Zeolites

		micropore diffusion at 24 °C[a]		micropore diffusion at 50 °C[a]	
zeolite	organic species	D/R^2 (min^{-1})	h	D/R^2 (min^{-1})	h
CBV-300	TCE	6.7×10^{-5}	0.63	9.5×10^{-5}	2.1
	2,2-DCP	4.1×10^{-5}	0.74	1.9×10^{-4}	2.1
	2-CP	1.9×10^{-3}	2.8	4.1×10^{-3}	1.7
CBV-720	2,2-DCP	1.0×10^{-2} [b]	–	9.8×10^{-2}	7.6
	2-CP	N/A[c]	–	5.0×10^{-3}	7.6
CBV-780	2,2-DCP	2.2×10^{-3} [b]	–	1.6×10^{-1}	20
	2-CP	N/A	–	5.8×10^{-2}	8.3

[a] Obtained by fitting experimental data with the RDM (*7*) unless indicated otherwise. A γ-distribution of diffusion rate constants was assumed to account for desorption from micropores with a wide distribution of sizes and properties, where D/R^2 is the mean micropore diffusion rate constant and η is the shape factor. [b] Obtained by fitting experimental data with the RDM coupled with the ADE (*7*) assuming a single micropore diffusion rate (D/R^2). [c] N/A: Not available because experimental data do not fit the desorption model (*7*).

data. On wet CBV-300, the D/R^2 values of 2-CP were 20−50 times higher than those of TCE and 2,2-DCP, in spite of their comparable molecular diffusivities in air and bulk water (Table 1). The relatively high D/R^2 of 2-CP appears to be an artifact stemming from rapid 2-CP formation near external surfaces. The kinetic desorption model assumes concentrations at the onset of desorption are uniform and independent of particle radius (*7*). In contrast, the relatively faster 2-CP formation near micropore openings (Figure 2) leads to a smaller average diffusion length (R) than that of 2,2-DCP, and fitting the desorption data to the RDM results in an anomalously high D/R^2.

The amount of TCE recovered from micropores of CBV-300 was 1.72 μmol/g (0.15 μL/g), which represents a very small fraction (0.03%) of the total micropore volume. The total amounts of 2,2-DCP and 2-CP recovered from the micropores of CBV-300 were 0.13 and 0.55 μmol/g, respectively (Table 2). This means that of the total 2,2-DCP (0.68 μmol/g) initially sorbed in the micropores 81.5% was transformed at 50 °C in 10 h, significantly less than the >99.85% predicted for bulk water under these conditions (*16*). In a preliminary experiment (data not shown) we observed that a very small fraction of water (~0.5% v/v) was sufficient to promote the dehydrohalogenation of 2,2-DCP (in bulk phase). The overall ratio of water to 2,2-DCP in micropores of CBV-300 was approximately 6500:1 (V/V). A possible explanation for the observed inhibition is that water is predominantly bound to the polar sites (surface cation density: 2.07 sites/nm^2) and therefore less reactive. Another contributing factor for the apparent inhibition may be that in the completely filled micropores 2,2-DCP molecules are relatively immobile (*28*) and thus sterically hindered in reacting with water. Inhibition appeared to be less near the particle surface, perhaps because water was more abundant near micropore openings due to the presence of hydrophilic edges. After desorbing for about 100 min, the mass remaining of unreacted 2,2-DCP exceeded that of 2-CP, suggesting 2,2-DCP transformed more slowly deeper in the micropores.

3. Transformation of 2,2-DCP in the Hydrophobic Zeolites CBV-720 and CBV-780. In contrast to CBV-300, the mass remaining profiles of 2,2-DCP and 2-CP on the hydrophobic zeolites (Figure 4) decreased only gradually without the distinct transition from fast- to slow-desorption typical of low microporosity solids (*3*, *5*−*9*). On the hydrophobic zeolites where the fraction of VOCs sorbed in micropores is much larger than that sorbed external to micropores, the fast-desorbing fraction was obscured by the high flux from micropores, as was observed for TCE desorbing from high silica (Si/Al = 65) ZSM-5 (*7*). Evaluation of desorption data using the ADE coupled with the RDM indicates that in both cases desorption from micropores was limited by the high gas-phase concentrations in the interparticulate pore spaces. For 2-CP only the approximately first 100 min of desorption data fitted the model with D/R^2 values identical to those of 2,2-DCP (Table 3). Thereafter, 2-CP removal slowed compared to that of 2,2-DCP, which is interpreted as relatively slow 2-CP formation deeper in the micropore spaces. The micropore diffusion rate constant of 2,2-DCP at 24 °C was significantly slower for CBV-300 than for CBV-720 and CBV-780, probably because coordinated water in the micropore spaces restricted diffusion. The mass remaining profiles at 50 °C and 75 °C fitted the RDM with a γ-distribution of diffusion rate constants indicating intraparticulate mass transfer (i.e., micropore desorption) was limiting at concentrations below 10 μmol/L.

After treatment at 50 °C for 10 h, the total masses of 2,2-DCP and 2-CP desorbed from CBV-720 and CBV-780 were 569 and 38 μmol/g and 553 and 29 μmol/g, respectively, which accounted for more than 98% of the sorbed masses (Table 2). The lack of transition from fast- to slow-desorption on

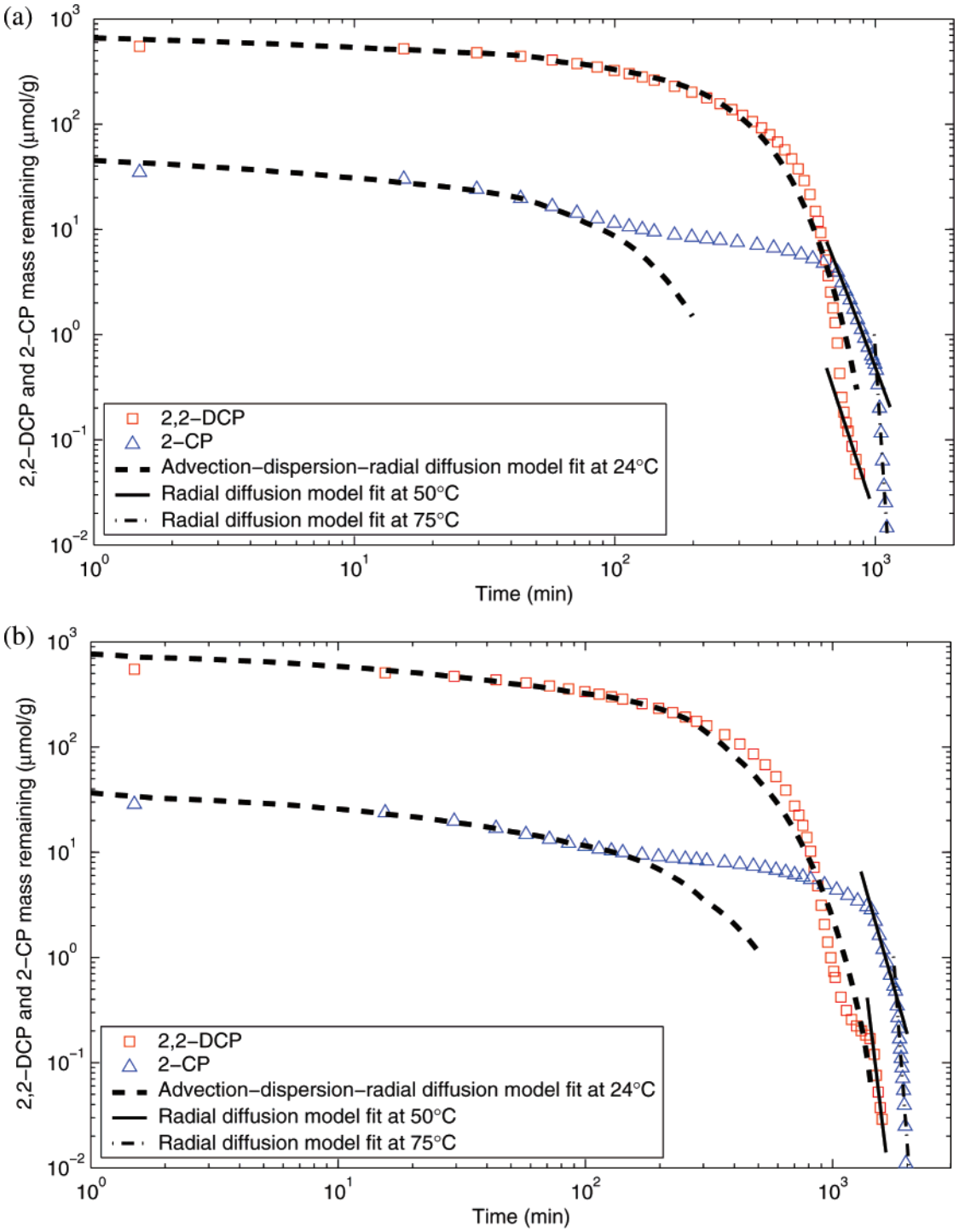

FIGURE 4. 2,2-DCP and 2-CP mass remaining profiles on (a) wet CBV-720 and (b) wet CBV-780 after 10 h reaction at 50 °C; lines represent model fits.

the hydrophobic zeolites (Figure S3, Supporting Information) indicates that essentially all 2,2-DCP molecules were sorbed inside micropores, leading us to conclude that only 6.3% and 5.0% 2,2-DCP transformed in micropores of wet CBV-720 and CBV-780, respectively. As expected, transformation of 2,2-DCP was significantly slower in the hydrophobic zeolites than in the hydrophilic CBV-300, where 81.5% of 2,2-DCP transformed in the micropores under the same conditions. In the micropores of wet CBV-720 and CBV-780, the volumes of water were approximately 6.4 times those of 2,2-DCP (molar ratios: ~36). Possible reasons for the observed inhibition were water limitation and perhaps also steric hindrance in the confined pore space, which reduced solvation of the transition state and the H^+ and Cl^- formed.

4. Distribution of 2,2-DCP Reactivity in Micropore Spaces. Figure 5 shows the molar fraction of 2,2-DCP ($f_{2,2-DCP} = C_{2,2-DCP}/(C_{2,2-DCP} + C_{2-CP})$) in the desorption flux from the hydrophilic and hydrophobic zeolites for the first 400 min. During removal of the fast-desorbing fraction, $f_{2,2-DCP}$ was approximately 0.9 in all three cases. Most of the 2,2-DCP molecules in this fraction resided as vapor in the interparticulate void space of the columns, and only a very small quantity of water was adsorbed on the external surface of the zeolites. Consequently, 2,2-DCP external to micropores

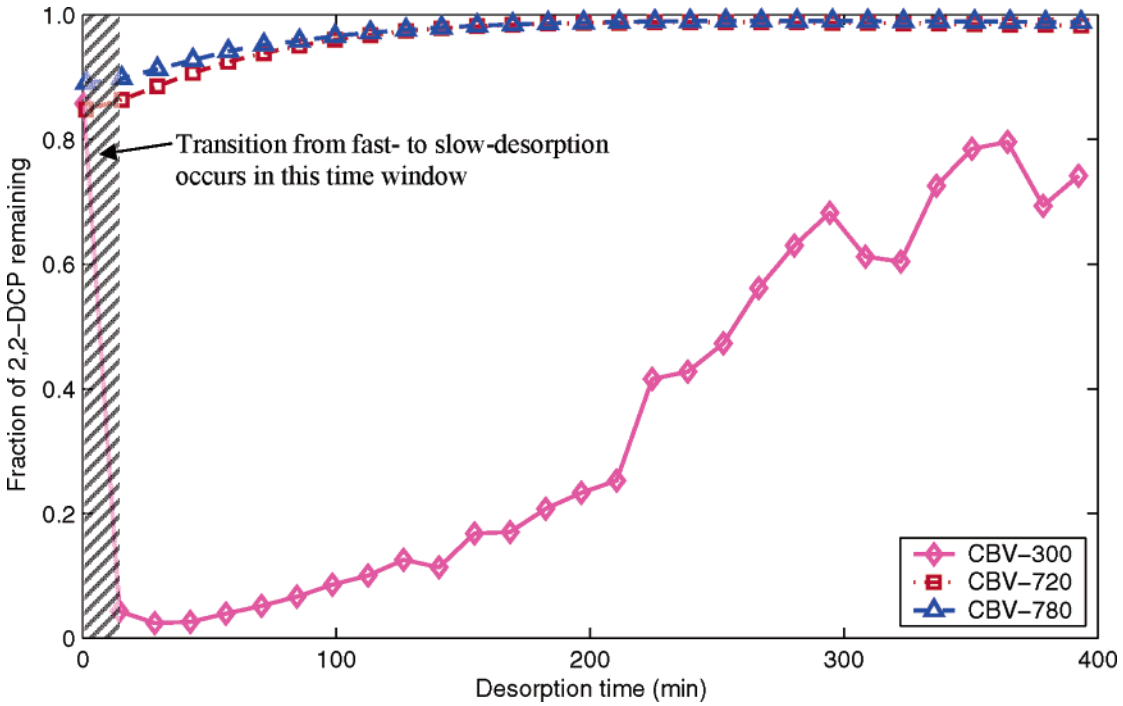

FIGURE 5. 2,2-DCP as a molar fraction of the total mass flux ($f_{2,2-DCP} = C_{2,2-DCP}/(C_{2,2-DCP} + C_{2-CP})$) during desorption after treating sorbed 2,2-DCP on wet Y zeolites (CBV-300, CBV-720, and CBV-780) at 50 °C for 10 h. Intermixing of 2,2-DCP remaining and 2-CP formed in the micropore spaces are negligible because of sorbate−sorbate interactions (*28*), and the molecules of 2,2-DCP and 2-CP are expected to have comparable diffusion rates during desorption. Therefore, the distribution of 2,2-DCP and 2-CP molecules along the diffusion paths within hydrophobic micropores can be approximated from the flux-time desorption profiles (Figures S2b and S3, Supporting Information).

transformed slowly due to the lack of water solvation in the gas phase (*18*).

Assuming the micropore spaces are emptied gradually from the pore openings inward and 2,2-DCP and 2-CP have identical diffusion rates, $f_{2,2-DCP}$ in the effluent stream may be taken as a measure of 2,2-DCP reactivity as a function of depth (Figure S4, Supporting Information). For the hydrophobic zeolites CBV-720 and CBV-780, $f_{2,2-DCP}$ increased from approximately 0.9 (at 15.5 min) to near 1 after 200 min of desorption and then stayed relatively constant. For the hydrophilic zeolite CBV-300, $f_{2,2-DCP}$ increased from approximately 0.04 after 14.5 min to the range of 0.6 to 0.8 in 300 min. The gradual increase in $f_{2,2-DCP}$ is consistent with relatively high abundance of water near the pore openings and a deficiency of reactive water at greater pore depth.

5. Implications for Degradation of Reactive Organic Contaminants in the Subsurface. The preservation of 2,2-DCP in the micropores of the three dealuminated Y zeolites is consistent with the hypothesis that the hydrolytic transformation of 2,2-DCP in hydrophobic micropores is inhibited. Because this reaction depends on the availability of free water, it can be expected that similar transformations that involve water, such as hydrolysis (via S_N1 or S_N2 mechanisms), substitution, and redox reactions, will be similarly inhibited. In geosorbent minerals, hydrophobic micropores are believed to exist in the pore spaces surrounded by uncharged siloxane surfaces (*3*, *21*), such as those created by stacking of the quasicrystals of clays (*14*, *25*). The reported reduced recovery and slower hydrolysis of chlorpyrifos in systems containing low concentrations of suspended smectites and river sediment (*2*) may be partially explained by sorption in the micropores present in the suspended solids (*14*, *25*). EDB, a soil fumigant that is poorly sorbed by soil, volatile, and easily biodegradable with a hydrolysis (uncatalyzed) half-life ranging from 2 to 4 years at 22−25 °C (*29*), has been found to persist in agricultural topsoils for decades (*4*), probably for the same reason.

Taken together, this study demonstrates that sorption in micropores can retard water-promoted reactions and that this phenomenon increases with the hydrophobicity of the micropores. If such hydrophobic micropores exist in geosorbents in significant quantities, reactive contaminants sequestered in them are likely to transform much slower than predicted by applying reaction rates derived from bulk aqueous solution data, leading to an underestimation of their environmental half-lives.

Acknowledgments

This study was funded by the U.S. Environmental Protection Agency under project R828772-01 through the Western Region Hazardous Substance Research Center. We are grateful to Dr. Pei C. Chiu, University of Delaware, for his input and to anonymous reviewers for helpful comments.

Supporting Information Available

Additional information on 2,2-DCP sorption breakthrough on the three zeolites, TCE desorption profile from CBV-300, 2,2-DCP and 2-CP desorption profiles from the three zeolites, 2,2-DCP transformation in the presence of tightly bound water and bulk water, effect of column heating and cooling on 2,2-DCP and 2-CP distribution, approximation for diffusion length during 2,2-DCP and 2-CP desorption, and the apparent normalized diffusion length scale for the first 400 min of desorption. This material is available free of charge via the Internet at http://pubs.acs.org.

Literature Cited

(1) Perdue, E. M.; Wolfe, N. L. Modification of pollutant hydrolysis kinetics in the presence of humic substances. *Environ. Sci. Technol.* **1982**, *16* (12), 847−852.
(2) Wu, J.; Laird, D. A. Hydrolysis of chlorpyrifos in aqueous and colloidal systems. *Isr. J. Chem.* **2002**, *42* (1), 99−107.
(3) Cheng, H.; Reinhard, M. Measuring hydrophobic micropore volumes in geosorbents from trichloroethylene desorption data. *Environ. Sci. Technol.* **2006**, *40* (11), 3595−3602.

(4) Steinberg, S. M.; Pignatello, J. J.; Sawhney, B. L. Persistence of 1,2-dibromoethane in soils: entrapment in intraparticle micropores. *Environ. Sci. Technol.* **1987**, *21* (12), 1201−1208.
(5) Werth, C. J.; Reinhard, M. Effects of temperature on trichloroethylene desorption from silica gel and natural sediments. 2. Kinetics. *Environ. Sci. Technol.* **1997**, *31* (3), 697−703.
(6) Werth, C. J.; Cunningham, J. A.; Roberts, P. V.; Reinhard, M. Effects of grain-scale mass transfer on the transport of volatile organics through sediments. 2. Column results. *Water Resour. Res.* **1997**, *33* (12), 2727−2740.
(7) Li, J.; Werth, C. J. Slow desorption mechanisms of volatile organic chemical mixtures in soil and sediment micropores. *Environ. Sci. Technol.* **2004**, *38* (2), 440−448.
(8) Grathwohl, P.; Reinhard, M. Desorption of trichloroethylene in aquifer material: rate limitation at the grain scale. *Environ. Sci. Technol.* **1993**, *27* (12), 2360−2366.
(9) Farrell, J.; Reinhard, M. Desorption of halogenated organics from model solids, sediments, and soil under unsaturated conditions. 2. Kinetics. *Environ. Sci. Technol.* **1994**, *28* (1), 63−72.
(10) Luthy, R. G.; Aiken, G. R.; Brusseau, M. L.; Cunningham, S. D.; Gschwend, P. M.; Pignatello, J. J.; Reinhard, M.; Traina, S.; Weber, W. J., Jr.; Westall, J. C. Sequestration of hydrophobic organic contaminants by geosorbents. *Environ. Sci. Technol.* **1997**, *31* (12), 3341−3347.
(11) Macalady, D. L.; Wolfe, N. L. Effects of sediment sorption and abiotic hydrolyses 1. organophosphorothioate esters. *J. Agric. Food Chem.* **1985**, *33* (2), 167−173.
(12) Haag, W. R.; Mill, T. Effect of a subsurface sediment on hydrolysis of haloalkanes and epoxides. *Environ. Sci. Technol.* **1988**, *22* (6), 658−663.
(13) Halasz, I.; Kim, S.; Marcus, B. Hydrophilic and hydrophobic adsorption on Y zeolites. *Mol. Phys.* **2002**, *100* (19), 3123−3132.
(14) Cheng, H.; Reinhard, M. Sorption of trichloroethylene in hydrophobic micropores of dealuminated Y zeolites and natural minerals. *Environ. Sci. Technol.* **2006**, *40* (24), 7694−7701.
(15) Ruthven, D. M. *Principles of Adsorption and Adsorption Processes*; John Wiley: New York, 1984; p 464.
(16) Jeffers, P. M.; Ward, L. M.; Woytowitch, L. M.; Wolfe, N. L. Homogeneous hydrolysis rate constants for selected chlorinated methanes, ethanes, ethenes, and propanes. *Environ. Sci. Technol.* **1989**, *23* (8), 965−969.
(17) Roberts, A. L.; Jeffers, P. M.; Wolfe, N. L.; Gschwend, P. M. Structure-reactivity relationships in dehydrohalogenation reactions of polychlorinated and polybrominated alkanes. *Crit. Rev. Environ. Sci. Technol.* **1993**, *23* (1), 1−39.
(18) Carey, F. A.; Sundberg, R. J. *Advanced Organic Chemistry, Part A: Structure and Mechanisms*, 4th ed.; Kluwer Academic Publishers: New York, 2000; p 823.
(19) Bartmess, J. E. Solvent effects on ion-molecule reactions. Vinyl anions vs. conjugate addition. *J. Am. Chem. Soc.* **1980**, *102* (7), 2483−2484.
(20) Caldwell, G. W.; Rozeboom, M. D.; Kiplinger, J. P.; Bartmess, J. E. Displacement, proton transfer, or hydrolysis? Mechanistic control of acetonitrile reactivity by stepwise solvation of reactants. *J. Am. Chem. Soc.* **1984**, *106* (3), 809−810.
(21) Farrell, J.; Hauck, B.; Jones, M. Thermodynamic investigation of trichloroethylene adsorption in water-saturated microporous adsorbents. *Environ. Toxicol. Chem.* **1999**, *18* (8), 1637−1642.
(22) Muller, E. A.; Gubbins, K. E. Molecular simulation study of hydrophilic and hydrophobic behavior of activated carbon surfaces. *Carbon* **1998**, *36* (10), 1433−1438.
(23) Muller, E. A.; Hung, F. R.; Gubbins, K. E. Adsorption of water vapor-methane mixtures on activated carbons. *Langmuir* **2000**, *16* (12), 5418−5424.
(24) Gregg, S. J.; Sing, K. S. W. *Adsorption, Surface Area and Porosity*; Academic Press: London, 1982; p 303.
(25) Hundal, L. S.; Thompson, M. L.; Laird, D. A.; Carmo, A. M. Sorption of phenanthrene by reference smectites. *Environ. Sci. Technol.* **2001**, *35* (17), 3456−3461.
(26) Fuerstenau, M. C.; Lopez-Valdiviezo, A.; Fuerstenau, D. W. Role of hydrolyzed cations in the natural hydrophobicity of talc. *Int. J. Mineral. Proc.* **1988**, *23* (3−4), 161−170.
(27) Yariv, S. Wettability of clay minerals. In *Modern Approaches to Wettability: Theory and Applications*; Schrader, M. E., Loeb, G. I., Eds.; Plenum Press: New York, 1992; p 279−326.
(28) Werth, C. J.; Reinhard, M. Counter-diffusion of isotopically labeled trichloroethylene in silica gel and geosorbent micropores: column results. *Environ. Sci. Technol.* **1999**, *33* (5), 730−736.
(29) Pignatello, J. J.; Cohen, S. Z. Environmental chemistry of ethylene dibromide in soil and ground water. *Rev. Environ. Contam. Toxicol.* **1990**, *112*, 1−47.
(30) Syracuse Research Corporation (SRC). *Physical/Chemical Property Database (PHYSPROP)*; SRC Environmental Science Center: Syracuse, NY, 1994.
(31) Dean, J. A. (Ed). *Lange's Handbook of Chemistry*, 15th ed.; McGraw-Hill: New York, 1999; p 1424.
(32) Perry, R. H., Green, D. W., Eds. *Perry's Chemical Engineers' Handbook*, 7th ed.; McGraw-Hill: New York, 1997; p 2581.
(33) Weber, W. J., Jr.; Huang, W. A distributed reactivity model for sorption by soils and sediments: 4. Intraparticle heterogeneity and phase-distribution relationships under nonequilibrium conditions. *Environ. Sci. Technol.* **1996**, *30* (3), 881−888.
(34) Ma, Y. C.; Foster, A. S.; Nieminen, R. M. Reactions and clustering of water with silica surface. *J. Chem. Phys.* **2005**, *122* (14), 1447091−14470.99.
(35) van Reeuwijk, L. P. *The thermal dehydration of natural zeolites*; H. Veenmanand Zonen B.V. Wageningen: The Netherlands: 1974; p 88.

Received for review September 29, 2006. Revised manuscript received December 20, 2006. Accepted December 24, 2006.

ES062332V